Brain Penetration and Efficacy of Different Mebendazole Polymorphs in a Mouse Brain Tumor Model

Ren-Yuan Bai[1], Verena Staedtke[2], Teresia Wanjiku[3], Michelle A. Rudek[3], Avadhut Joshi[1], Gary L. Gallia[1,3], and Gregory J. Riggins[1,3]

Abstract

Purpose: Mebendazole (MBZ), first used as an antiparasitic drug, shows preclinical efficacy in models of glioblastoma and medulloblastoma. Three different mebendazole polymorphs (A, B, and C) exist, and a detailed assessment of the brain penetration, pharmacokinetics, and antitumor properties of each individual mebendazole polymorph is necessary to improve mebendazole-based brain cancer therapy.

Experimental Design and Results: In this study, various marketed and custom-formulated mebendazole tablets were analyzed for their polymorph content by IR spectroscopy and subsequently tested in an orthotopic GL261 mouse glioma model for efficacy and tolerability. The pharmacokinetics and brain concentration of mebendazole polymorphs and two main metabolites were analyzed by LC/MS. We found that polymorph B and C both increased survival in a GL261 glioma model, as B exhibited greater toxicity. Polymorph A showed no benefit. Polymorph B and C both reached concentrations in the brain that exceeded the IC_{50} in GL261 cells 29-fold. In addition, polymorph C demonstrated an AUC_{0-24h} brain-to-plasma (B/P) ratio of 0.82, whereas B showed higher plasma AUC and lower B/P ratio. In contrast, polymorph A presented markedly lower levels in the plasma and brain. Furthermore, the combination with elacridar was able to significantly improve the efficacy of polymorph C in GL261 glioma and D425 medulloblastoma models in mice.

Conclusion: Among mebendazole polymorphs, C reaches therapeutically effective concentrations in the brain tissue and tumor with fewer side effects, and is the better choice for brain cancer therapy. Its efficacy can be further enhanced by combination with elacridar. *Clin Cancer Res; 1–9. ©2015 AACR.*

Introduction

Central nervous system (CNS) cancers are difficult to treat because most systemically administered therapeutics fail to reach effective concentrations in intracranial tumors (1). This is partially explained by the blood–brain barrier (BBB). In the CNS, the BBB exists along all capillaries consisting of tight junctions, thereby blocking large and hydrophilic molecules from passing to the CNS tissues. It is estimated that only about 2% of small-molecule drugs are able to effectively cross the BBB (2).

Mebendazole (MBZ) has been safely used as an antiparasitic in humans for over four decades and displays efficacy against intracranial helminthic infections. We recently demonstrated mebendazole preclinical efficacy in orthotopic glioma and medulloblas-

toma rodent models (3, 4). Mebendazole significantly reduced tumor growth and improved survival of brain tumor-bearing mice. On the basis of these results, a phase I clinical trial with a dose escalation of mebendazole for newly diagnosed high-grade glioma patients has been initiated (NCT01729260). Evidence has been generated supporting several anticancer mechanisms for mebendazole, including tubulin-binding, kinase inhibition, anti-angiogenesis, proapoptosis, and inhibition of the hedgehog pathway (3, 5–9). However, the important features of mebendazole's brain penetration and pharmacokinetics remain to be determined. This understanding is important to potentially improve the clinical use of mebendazole.

Mebendazole is highly hydrophobic and can form three different polymorphs based on crystallization conditions (10). The polymorphs A, B, and C (MBZ-A, B, and C) displayed distinct features in solubility, toxicity and therapeutic effects in anthelmintic applications (11–13). The difference in antitumor efficacy of the three polymorphs has not yet been investigated; however, this information might be crucial to future mebendazole cancer therapies, because drug formulations might contain various polymorphs in different amounts or combinations. Another critical reason for further investigation is that polymorph C, the most efficacious polymorph in anthelmintic use, can transform over time to the less effective polymorph A, especially with higher temperatures and humidity (14). Mebendazole polymorphs are three different solid forms that occur depending on which solvent is used during the crystallization of the synthesis process. These structural distinctions in the solid phase disappear once mebendazole is dissolved. The variable pharmaceutical properties of

[1]Department of Neurosurgery, Johns Hopkins University School of Medicine, Baltimore, Maryland. [2]Department of Neurology, Johns Hopkins University School of Medicine, Baltimore, Maryland. [3]Sidney Kimmel Comprehensive Cancer Center, Johns Hopkins University School of Medicine, Baltimore, Maryland.

Note: Supplementary data for this article are available at Clinical Cancer Research Online (http://clincancerres.aacrjournals.org/).

R.Y. Bai and V. Staedtke contributed equally to this article.

Corresponding Authors: Ren-Yuan Bai and Gregory J. Riggins, Department of Neurosurgery, Johns Hopkins University, 1550 Orleans Street, Room 257 CRBII, Baltimore, MD 21161. Phone: 410-502-2907; Fax: 410-502-5559; E-mail: rbai1@jhmi.edu or griggin1@jhmi.edu

Translational Relevance

Mebendazole is an antiparasitic drug with over 40 years of safe use. We recently repurposed mebendazole for glioblastoma therapy and launched a phase I trial. In preclinical studies, mebendazole increases survival in multiple orthotopic glioma and medulloblastoma models. Three polymorphs of mebendazole exist, but the relative polymorph content for existing drugs varies, and the therapeutic relevance of the different polymorphs to anticancer activity is unknown. We show that as an oral drug mebendazole polymorph C is superior form and it reaches the brain and brain tumors in effective concentrations. Efficacy was further improved by combining mebendazole with elacridar. We recommend using pure polymorph C for future brain cancer clinical trials, possibly in combination with elacridar.

mebendazole polymorphs are likely the result of different solubility and bioavailability of each polymorph. Because the polymorphs only exist in the solid form and mebendazole is exclusively an oral drug, studying the relevant antitumor properties of different polymorphs is best accomplished by determining bioavailability and efficacy in animal models via oral administration of mebendazole polymorphs.

In this work, we studied pharmacokinetics of MBZ-A, B, and C and their concentrations in the brain following the oral administration. We focused our investigation on the brain and brain tumor distributions of MBZ-C, the polymorph found most commonly in the generic mebendazole tablets, as well as the levels of mebendazole metabolites. To determine whether we could further improve mebendazole efficacy, we also investigated the use of a P-glycoprotein inhibitor in combination with mebendazole.

Materials and Methods

Chemicals and drugs

Mebendazole tablets (500 mg) from Janssen Pharmaceuticals (Pantelmin) and Medley Pharmaceuticals were purchased from local pharmacies in Brazil in 2013 and stored at $-20°C$ freezer. Mebendazole tablets (100 mg) from Teva Pharmaceuticals USA were purchased from the Outpatient Pharmacy at the Johns Hopkins Hospital in 2011 and stored at room temperature (RT). Teva has discontinued mebendazole in the U.S. market since October 2011. Aurochem Laboratories Ltd. manufactured mebendazole tablets (500 mg), S2015 containing the current active pharmaceutical ingredient (API) that typically has mixed polymorphs, and S2017 (polymorph C) with specific API revealed, which is the formulation used in the current phase I clinical trial (NCT01729260). Aurochem also kindly supplied us with mebendazole polymorph A, B, and C. Elacridar [GF120918; N-(4-(2-(1,2,3,4-tetrahydro-6,7-dimethoxy-2-isoquinolinyl)ethyl)phenyl)-9,10-dihydro-5-methoxy-9-oxo-4-acridine carboxamide)] was purchased from Sigma. Thiabendazole, flubendazole, oxifendazole, and fenbendazole were purchased from Sigma.

Cell lines and tissue culture

Mouse glioma cell line GL261 cells were kindly provided by Dr. Michael Lim's laboratory at the Johns Hopkins University in 2009, and human medulloblastoma cell line D425Med (D425) was obtained from the Duke University Brain Tumor Center without further authentication (3, 15). GL261 and D425 cells were maintained in DMEM media supplemented with 10% FBS and antibiotics at $37°C$ in humidified air containing 5% CO_2. GL261-luc cells expressing firefly luciferase were described previously (3).

Cell growth assays

The viable cells were measured with Cell Counting Kit-8 (Dojindo Molecular Technology) containing WST-8 at 450 nm on a PerkinElmer VICTOR3 plate reader. IC50s measurements were performed by incubating cells at a range of concentrations for 72 hours and calculated by GraphPad Prism 5.0 using the log (inhibitor) versus response function and nonlinear fit.

Infrared spectrometry of mebendazole polymorphs

A Direct Detect IR spectrometer was used (Millipore). Mebendazole powder or tablets ground to powder was mixed with water first, applied to the card, and air dried following the manufacturer's instructions. The spectra of $-C=O$ and $-NH$ were analyzed and compared as described before (10).

Intracranial mouse models

All animal studies were approved by the Animal Care and Use Committee (ACUC) of the Johns Hopkins University. The intracranial implantation of GL261-luc in the frontal lobe and D425 cells in the cerebellum of the mouse brain followed the procedure described before (3, 4). Five days after tumor implantation, mice were gavaged with mebendazole or the other benzimidazoles at 50 mg/kg daily for the first 20 days and then 5 days a week as described before for single drug treatment (3). Mebendazole and other benzimidazoles were prepared by either mixing the power with PBS and sesame oil (1:1, v:v; Sigma) or by grinding the tablets to powder and resuspending in the aforementioned PBS/sesame oil mixture. Elacridar was prepared as a 10 mg/mL suspension in 0.5% hydroxypropylmethylcellulose and 0.5% Tween 80 in PBS similarly as described before (16).

Mebendazole pharmacokinetic studies

Female C57BL6 mice, 5 to 6 weeks of age, were purchased from NCI. Animal experimentation was conducted under an approved IACUC protocol and complied with local and national guidelines. All mebendazole polymorphs were administered by oral gavage at a dose of 50 mg/kg. Elacridar was administered by oral gavage at 50 mg/kg 2 hours before the administration of MBZ-C. Mice (3 animals/time point) were first anesthetized via i.p. injection of 60 μL of a stock solution containing ketamine hydrochloride (75 mg/kg; 100 mg/mL; Ketamine HCl; Abbot Laboratories) and xylazine (7.5 mg/kg; 100 mg/mL; Xyla-ject; Phoenix Pharmaceutical, St. Joseph) in a sterile 0.9% NaCl solution. Then the blood samples were taken by puncturing and aspiring from the left heart ventricle. Blood samples were mixed with 5 mmol/L EDTA and centrifuged at $10,000 \times g$ for 5 minutes to obtain the plasma for further analysis.

For brain distribution studies, mice were perfused under anesthesia with 20 mL ice-cold saline supplemented with 20 μL of 0.02% heparin by injecting slowly into the left heart ventricle using a 20-gauge needle. The right atrium was cut open before to allow the blood outflow. The yellow color of kidney indicated a good perfusion quality that was essential to deplete blood from the brain tissue. In GL261 tumor-bearing mice, GL261 tumor was distinguished from the normal brain by easily recognizable

differences in color and shade. GL261 tumor was separated with a scalpel and the normal brain tissue was cut from the contralateral hemisphere. All brain samples were weighed and stored at -80°C before processing.

Blood, brain, and brain tumor tissues were harvested as a function of time after mebendazole administration. To compare the pharmacokinetics of mebendazole polymorphs, three cohorts of mice each were administered a single dose of 50 mg/kg by oral gavage. For the initial comparison studies, plasma samples were obtained at 1, 2.5, 4, 6, 8, 15, and 24 hours after mebendazole administration whereas brain tissue was only collected at 6 hours. For the comparison studies of polymorph C with or without elacridar, plasma and brain tissue samples were obtained at 2.5, 4, and 8 hours after mebendazole administration. Brain tumor tissue samples were also obtained for polymorph C alone.

Measurement of mebendazole and metabolites

Mebendazole and the two metabolites, 2-amino-5-benzoyl-benzimidazole (MBZ-NH$_2$, CAS 52329-60-9) and rac dihydro mebendazole (MBZ-OH, CAS 60254-95-7), were quantified in plasma, brain, and brain tumor tissue. Tissue homogenates were prepared at a concentration of 200 mg/mL in plasma before extraction. Mebendazole and metabolites were extracted from 50 μL of plasma or tissue homogenates with 0.1 mL of methanol containing 0.5 μg/mL of the internal standard A620223.69. After centrifugation, the supernatant (60 μL) was mixed with water (40 μL), and then transferred into autosampler vials. Separation was achieved with an Atlantis dC18 (2.1 × 100 mm, 3 μm) column at RT with methanol/water mobile phase (60:40, v:v) containing 0.1% formic acid using isocratic flow at 0.25 mL/min for 5 minutes. The analytes were monitored using an AB Sciex triple quadrupole 5500 mass-spectrometric detector (Applied Biosystems) using electrospray ionization operating in positive mode. The spectrometer was programmed to allow the (MH$^+$) ions of MBZ, MBZ-NH$_2$, MBZ-OH, and A620223.69 at m/z 296.0, 238.0, 298.0, and 287.2, respectively, to pass through the first quadrupole (Q1) and into the collision cell (Q2). The daughter ions for MBZ (m/z 263.9), MBZ-NH$_2$ (m/z 105.1), MBZ-OH (m/z 266.0), and A620223.69 (m/z 124.1) were monitored through the third quadrupole (Q3). Calibration curves for mebendazole and metabolites were computed using the area ratio peak of the analysis to
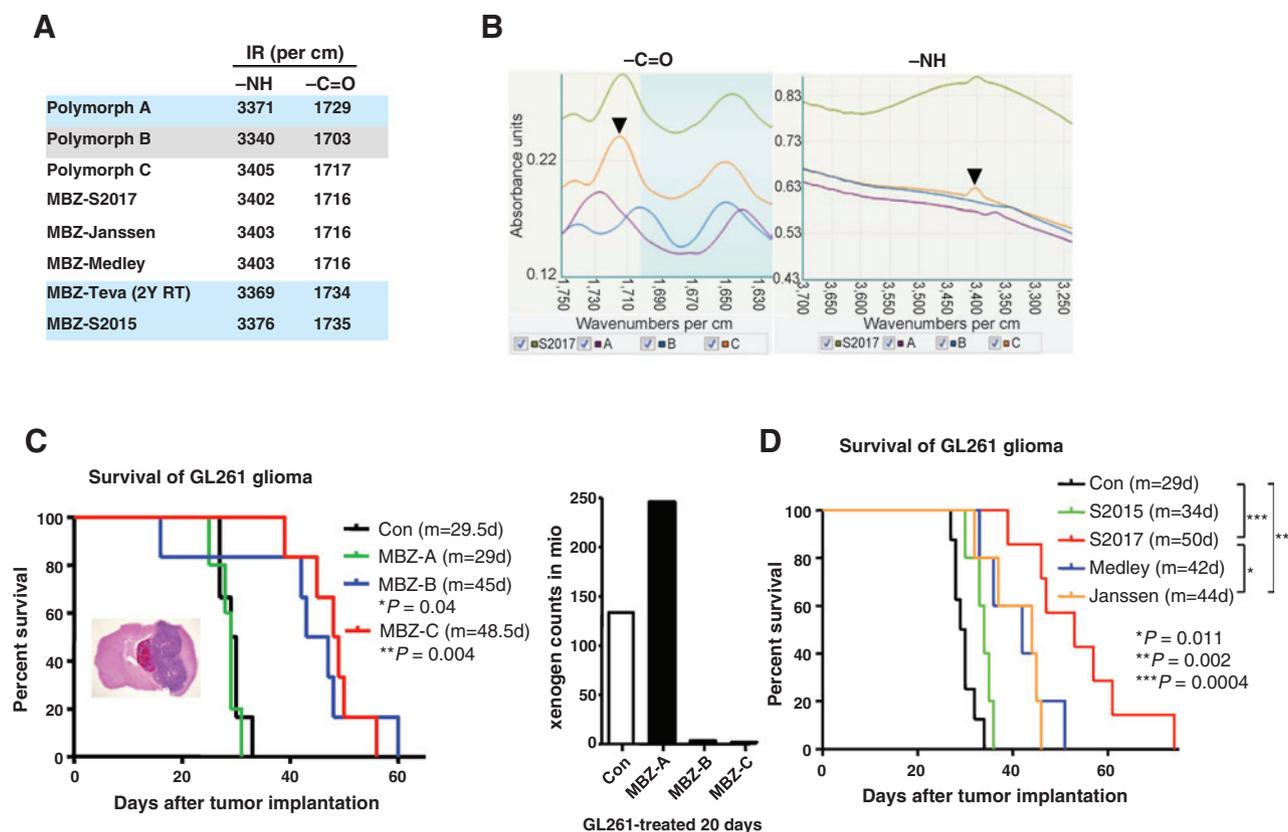
Figure 1.
MBZ-C is the most efficacious polymorph with limited toxicity. A and B, IR spectra of mebendazole (MBZ) polymorphs and mebendazole tablets from different suppliers: S2015 and S2017 (Aurochem), Teva (after 2-year storage at RT), Medley and Janssen. Two peaks represent the –NH and –C = O groups in the molecules. Black arrow heads indicate the peaks of MBZ-C control. C, left, Kaplan–Meier survival curves of mice implanted with GL261-luc glioma and treated with different mebendazole polymorphs (A–C). A hematoxylin and eosin (H&E) staining of the GL261-luc glioma-bearing mouse brain by coronal cut was shown. Five days after the tumor implantation, the mice were gavaged with mebendazole and control animals were feed with vehicles. One mouse in the MBZ-B group presumably died from drug toxicity as no significant tumor was found in the brain. The P values of Con versus MBZ-B and Con versus MBZ-C are indicated. The P value of MBZ-B versus MBZ-C is 0.72; m, median survival in days; Con, $n = 6$; MBZ-A, $n = 5$; MBZ-B, $n = 6$; MBZ-C, $n = 6$. Right, luciferase counts measured by Xenogen reflected the size of GL261-luc brain tumor in mice treated with mebendazole polymorphs for 20 days. D, survival curves of GL261-luc–bearing mice treated with mebendazole tablets from different suppliers; Con, $n = 6$; S2015, $n = 5$; S2017, $n = 6$; Medley, $n = 5$; Janssen, $n = 5$.

Bai et al.

the internal standard by using a quadratic equation with a 1/x weighting function over the range of 5 to 500 ng/mL (mebendazole) and 1 to 500 ng/mL (metabolites) with dilutions of up to 1:100 (v:v). If one or more concentrations were below limits of quantification, a value of half the limit of quantification was assigned for pharmacokinetic calculations. If two consecutive time points were below limits of quantification, the last one was excluded from the analysis.

Mean plasma and brain concentrations were calculated at each time point for both mebendazole and its metabolites. 1.045 g/mL was used as the average wet rodent brain tissue density (17). Pharmacokinetic parameters were calculated from mean mebendazole and its metabolites concentration-time data using noncompartmental methods as analyzed in Phoenix WinNonlin version 6.3 (Pharsight Corp.). C_{max} and T_{max} were the observed values from the mean concentration data. The AUC_{last} was calculated using the log-linear trapezoidal method. λ_z was determined from the slope of the terminal phase of the concentration-time profile. The terminal half-life ($T_{1/2}$) was determined by dividing 0.693 by λ_z. If the r^2 of λ_z was <0.9, the $T_{1/2}$ was not reported. Relative systemic exposure to mebendazole was calculated using the AUC_{last}:Metabolites AUC_{last}/MBZ AUC_{last}. Relative systemic exposure in brain or brain tumor compared with plasma was calculated using the AUC_{last}:Brain or Brain Tumor AUC_{last}/Plasma AUC_{last}.

Statistical analysis

Animal survival data were analyzed by GraphPad Prism 5.0. The P values were determined by a Mantel–Cox test. A P value under 0.05 was accepted as statistically significant.

For the pharmacokinetic studies comparing the polymorphs or administration with elacridar, the Method of Bailer was used to estimate the variance of AUC_{last} given the calculated variance of the mean concentration at each time point (18). This was then followed by a pairwise comparison using a Z-test to determine whether there was a significant difference between mebendazole exposure as expressed by AUC_{last} (19). Comparisons of individual data were conducted using the nonparametric Wilcoxon signed-rank rank test with post hoc analysis using an All Pairs Tukey–Kramer test. The level of significance was $P < 0.05$.

Results

Polymorph C was most effective for treating brain tumors in mice

We examined the polymorph content of several commercially available tablets (Janssen, Medley, and Teva) and two made to
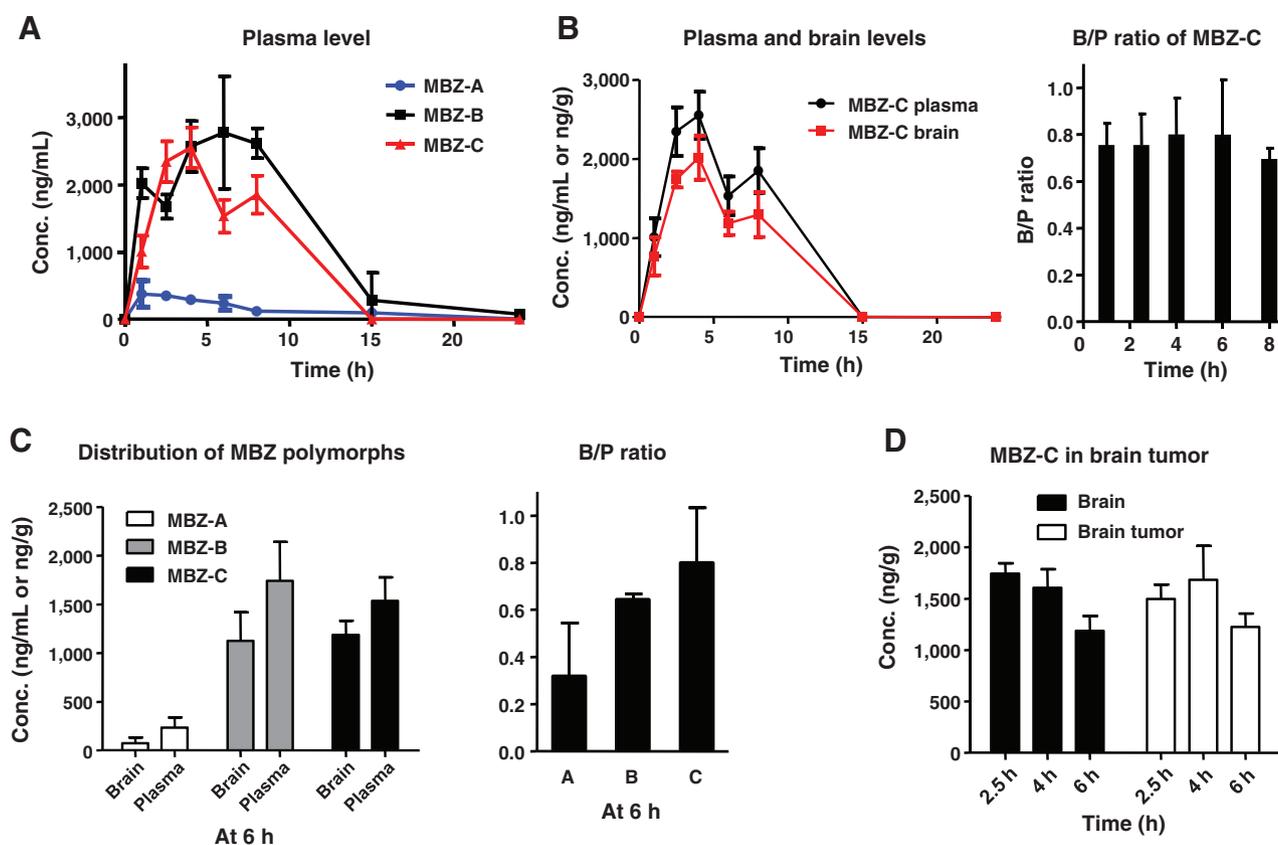
Figure 2.
Plasma and brain distributions of mebendazole (MBZ) polymorphs. A, a time course of the mebendazole plasma levels in C57BL6 mice after oral gavage of MBZ-A, B, or C at 50 mg/kg. B, left, brain and plasma levels of MBZ-C in a time course after oral gavage at 50 mg/kg. Animals were thoroughly perfused with PBS for all brain distribution studies. Right, brain/plasma (B/P) ratios of MBZ-C. Data were collected from three mice at each time point. C, left, brain and plasma levels of mebendazole polymorphs at 6 hours following oral gavage (50 mg/kg). B/P ratio of mebendazole polymorphs at 6 hours following oral gavage. Right, the mean B/P ratio of MBZ-A is 0.32, MBZ-B is 0.64, and MBZ-C is 0.80. D, MBZ-C distributed equally in the brain and brain tumor. GL261 tumors implanted in the right side of mouse frontal lobe were resected and compared with the contralateral normal brain tissue.

order tablets (Aurochem S2015 used the current API that typically has mixed polymorphs and S2017 was specified as pure MBZ-C) by comparing their IR profiles with the individual mebendazole polymorphs (Fig. 1A and B). On the basis of the IR peaks of –C= O and –NH bonds, we determined that the Janssen and Medley tablets were made of mainly MBZ-C as well as the Aurochem S2017. Aurochem S2015 and Teva tablets that have been stored at RT for 2 years showed mainly the profiles of MBZ-A. As a control, polymorph A, B, and C were dissolved in DMSO and incubated individually with GL261 glioma cells, which showed equal cytotoxicity (data not shown).

MBZ-A appeared to be ineffective in treating intracranial GL261 glioma-bearing mice, whereas MBZ-C displayed the best efficacy (Fig. 1C). Although MBZ-B showed a similar survival to MBZ-C, it caused more toxicity with 1 treatment-related death among 6 treated mice (Fig. 1C, left) and loss of body weight (Supplementary Fig. S1). The efficacy data reflected the polymorph composition of mebendazole tablets well in the sense that S2015 was ineffective and other tablets made of MBZ-C all showed significant efficacy by extending the mean survival to 42 to 50 days from 29 days of the control group (Fig. 1D).

Mebendazole reached the brain at significant levels

Following an oral dosing of 50 mg/kg, MBZ-C achieved a plasma AUC_{0-24h} of 16,039 h*ng/mL (Fig. 2A and Table 1). In comparison, MBZ-B reached a plasma AUC_{0-24h} of 26,474 h*ng/ mL, whereas MBZ-A plasma AUC_{0-24h} reached only 3,052 h*ng/ mL, by far the lowest among all three polymorphs ($P < 0.05$ for AUC_{0-24h} with MBZ-B>-C>-A; Table 1). Measurements of brain tissues following a thorough perfusion revealed significant presence of MBZ-C over a time course, correlating closely with the plasma mebendazole levels with a brain/plasma (B/P) ratio of 0.75 on average that remained relatively stable during the 8 hours (Fig. 2B). Comparing the polymorphs at 6 hours following oral gavage, we found that MBZ-C and -B achieved similar brain levels,

despite MBZ-B's higher levels and AUC_{0-24h} in the plasma (Fig. 2C, left and Table 1), resulting in a slightly favorable mean B/P ratio of MBZ-C over MBZ-B (0.80 for C vs. 0.64 for B and 0.29 for A, $P = 0.055$; Fig. 2C, right). This corroborates well with the efficacy data in Fig. 1C, where MBZ-B and -C demonstrated similar survival benefit in the GL261 model (mean survival, 45 days of MBZ-B vs. 48.5 days of MBZ-C). However, it is notable that MBZ-B displayed greater toxicity, resulting in early death of one mouse among the six treated animals (Fig. 2C, left). Analysis of the GL261 brain tumor and the contralateral brain tissues indicated equal distribution of MBZ-C in the brain tumor and the normal brain tissues (Fig. 2D).

Pharmacokinetics of mebendazole metabolites

We determined the plasma levels of the major metabolites $MBZ-NH_2$ and MBZ-OH of mebendazole polymorphs ($P < 0.05$ for AUC_{0-24h} of $MBZ-NH_2$ with MBZ-B>C>A; $P < 0.05$ for AUC_{0-24h} of MBZ-OH with MBZ-B and C>A; Table 1). The levels of MBZ-C's metabolites in plasma and brain generally followed the same pattern of MBZ-C's concentration (Fig. 3A and B). $MBZ-NH_2$ showed higher levels than MBZ-OH in the plasma (Fig. 3A), with an AUC_{0-24h} of 10,516 h*ng/mL compared with 5,781 h*ng/mL of MBZ-OH (Table 1). Notably, in a reversed pattern, $MBZ-NH_2$ was measured at much lower levels than MBZ-OH in the brain in terms of C_{max} and AUC_{0-24h} (Fig. 3B and Table 1). Interestingly, $MBZ-NH_2$ reached significantly higher levels in GL261 glioma than in the contralateral brain (Fig. 3C). To elucidate the antitumor role of mebendazole metabolites, we compared the IC_{50} of mebendazole, MBZ-OH and $MBZ-NH_2$ in GL261 cells and determined $MBZ-NH_2$ is the least cytotoxic derivative of mebendazole *in vitro* (Fig. 3D).

Combination of mebendazole with elacridar

Achieving a sufficient therapeutic concentration in the tumor and the surrounding brain tissue is a critical challenge that is faced

Table 1. Pharmacokinetics of mebendazole polymorphs in mice

Polymorph	Detection	Plasma $T_{1/2}$ (h)	T_{max} (h)	C_{max} (ng/mL)	AUC_{0-24h} (h*ng/mL)	Brain $T_{1/2}$ (h)	T_{max} (h)	C_{max} (ng/g)	AUC_{0-24h} (h*ng/g)	B/P
A	MBZ	3.23	1	379.3	3,052					
B	MBZ	3.18	6	2,778.3	26,474					
C	MBZ	0.90	4	2,553.3	16,039	1.64	4	2,016	13,134	0.82
A	$MBZ-NH_2$		2.5	201.3	2,841					
B	$MBZ-NH_2$		8	1,656.7	18,583					
C	$MBZ-NH_2$		8	1,416.7	10,516		8	201.6	1,336	0.13
A	MBZ-OH		1	32.1	247					
B	MBZ-OH		8	744.7	4,970					
C	MBZ-OH		6	951.7	5,781		8	794.3	5,427	0.94

Drug	Detection	Plasma T_{max} (h)	C_{max} (ng/mL)	AUC_{0-8h} (h*ng/mL)	Brain T_{max} (h)	C_{max} (ng/g)	AUC_{0-8h} (h*ng/g)	B/P AUC_{0-8h}	Significant?
MBZ	MBZ	4	2,553.3	15,340	4	2016.0	11,510	0.75	
ELD+MBZ	MBZ	2.5	1,433.3	8,636	2.5	1459.7	8,904	1.03	No
MBZ	$MBZ-NH_2$	8	1,416.7	8,264	8	201.6	1,010	0.12	
ELD+MBZ	$MBZ-NH_2$	2.5	1,191.7	7,826	8	387.8	2,386	0.30	Yes
MBZ	MBZ-OH	2.5	810.0	4,679	8	794.3	4,135	0.88	
ELD+MBZ	MBZ-OH	2.5	491.0	2,680	2.5	712.6	3,475	1.30	No

NOTE: Top section, using LS/MS, mebendazole, and the metabolites $MBZ-NH_2$ and MBZ-OH were measured in plasma samples of mice orally gavaged with the indicated mebendazole polymorphs. In terms of the plasma AUC_{0-24h}, it is B>C>A with $P < 0.05$. Bottom section, pharmacokinetics of MBZ-C and metabolites in mice gavaged with mebendazole or the combination of mebendazole and elacridar (ELD).
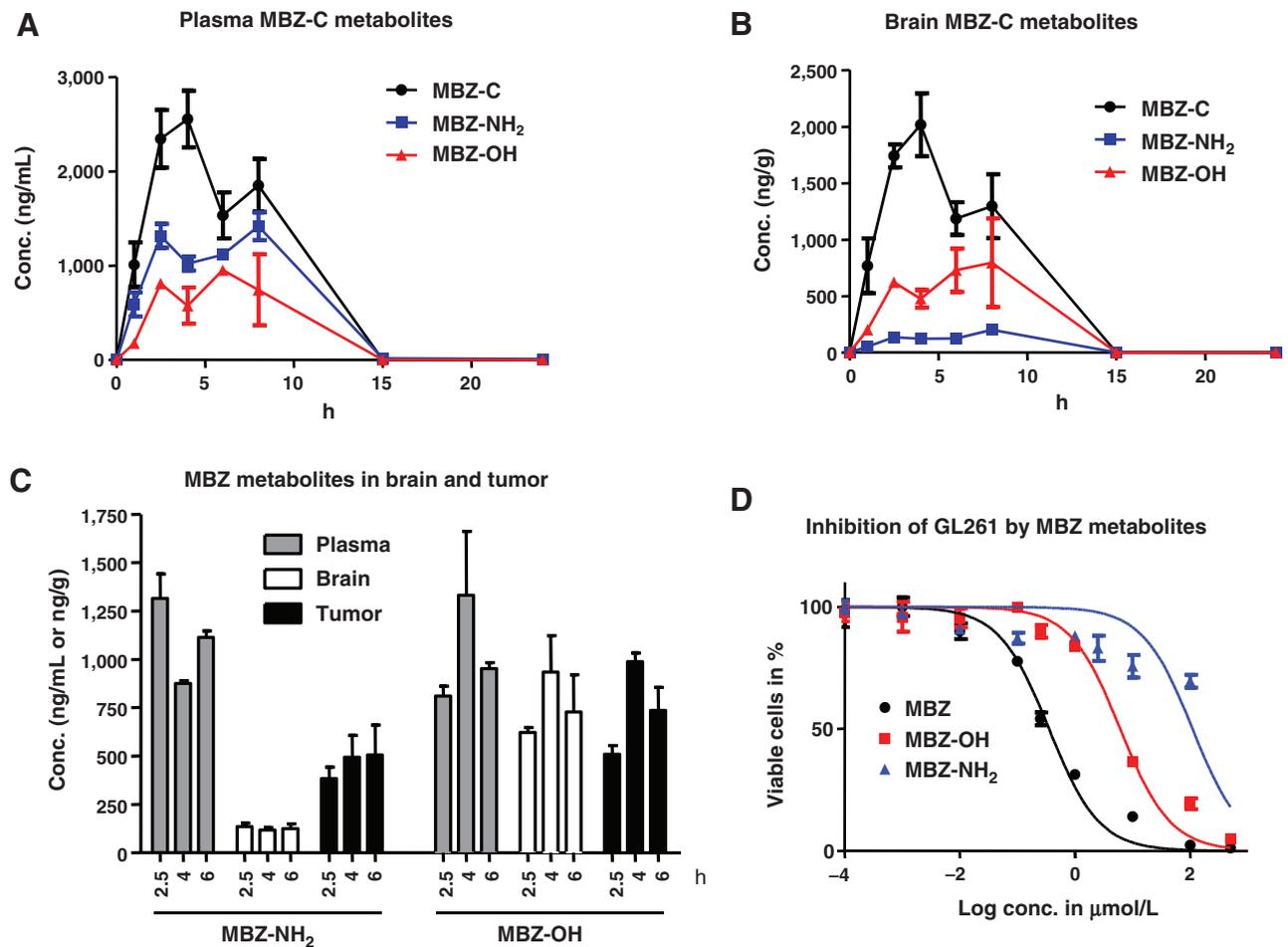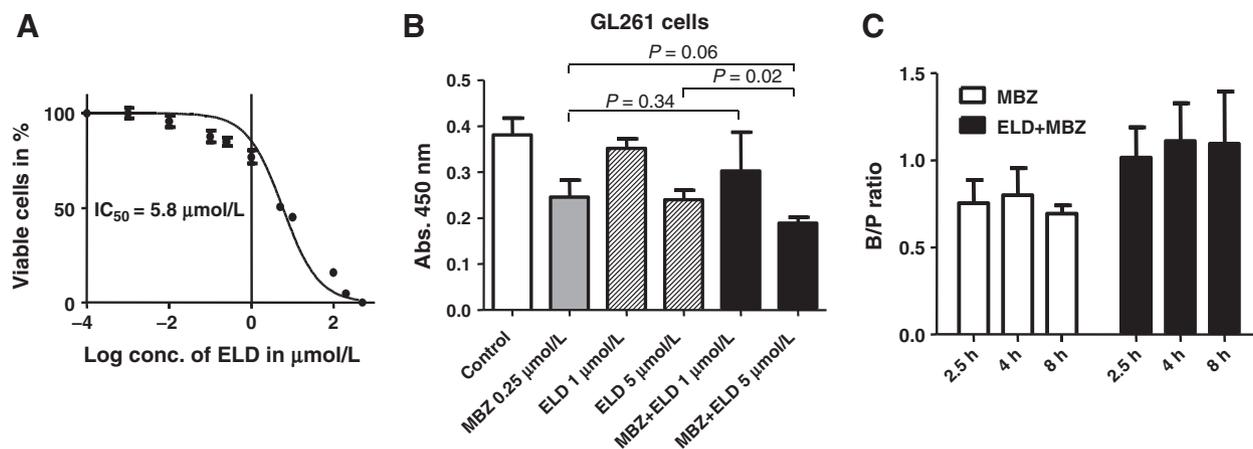
Figure 3.
Distribution of mebendazole (MBZ) metabolites. A and B, the plasma and brain levels of mebendazole and its metabolites, MBZ-OH (rac dihydro mebendazole, CAS 60254-95-7) and MBZ-NH$_2$ (2-amino-5-benzoyl-benzimidazole, CAS 52329-60-9), were analyzed following oral gavage of 50 mg/kg MBZ-C. C, the distributions of mebendazole metabolites in the plasma, brain, and GL261 brain tumor. At 2.5, 4, and 6 hours after oral gavage of MBZ-C, mice implanted with GL261 for 25 days were sacrificed and the blood, GL261 brain tumor and contralateral normal brain tissues were sampled and analyzed. D, an IC$_{50}$ curve of GL261 glioma cells with mebendazole and metabolites. GL261 cells were incubated with mebendazole or its metabolites for 72 hours and the living cells were measured.

by almost all brain cancer therapies. Four hours after oral administration, we found MBZ-C brain concentration peaked at 2,016 ng/g (equivalent to 7.1 μmol/L; Table 1), which was well above the IC$_{50}$s of cultured glioma and medulloblastoma cells (0.11–1 μmol/L) and also above mebendazole's inhibitory IC$_{50}$ with VEGFR2 kinase at 4.3 μmol/L in $vitro$ (3, 4). The relatively high brain concentration might help explain mebendazole efficacy in brain tumor models. Next, we reasoned that a further increase in the brain distribution of mebendazole would be desirable as it may increase therapeutic efficacy. Aside from a pure mechanical barrier, the BBB uses active efflux mechanisms to limit drug entry such as P-glycoprotein (P-gp). Elacridar is a potent third-generation inhibitor that inhibits P-gp as well as breast cancer resistance protein (BCRP), and coadministration of elacridar has increased the brain penetration of several drugs (16, 20). We first examined the cytotoxicity of elacridar in GL261 mouse glioma cells and determined the IC$_{50}$ to be 5.8 μmol/L (Fig. 4A). Combining elacridar with 0.25 μmol/L mebendazole only marginally increased the cytotoxicity in $vitro$ (Fig. 4B). Oral administration of 50 mg/kg elacridar 2 hours before MBZ-C did not significantly

change the brain concentration of mebendazole in terms of AUC$_{0-8h}$, whereas B/P ratio average of 2.5, 4, and 8 hours was shifted slightly higher from 0.75 to 1.03, which, however, was not statistically significant (Table 1 and Fig. 4C). Interestingly, this was accompanied by a significant increase in MBZ-NH$_2$ along with an elevation of the B/P ratio from 0.12 to 0.30 in the brain when treated with a combination of elacridar and MBZ-C (Table 1).

Combination with elacridar improved the treatment of mebendazole

Combination therapy of elacridar and mebendazole increased the survival benefit in GL261 syngeneic glioma and D425 xenograft medulloblastoma models (Fig. 5). This was achieved by adding 7 or 14 days of 50 mg/kg elacridar treatment to the standard mebendazole (MBZ-C) regimen of 50 mg/kg. Specifically, in GL261, combination therapy improved the median survival to 92.5 and 110.5 days dependent on the treatment length, which is a stark increase from 53 days of mebendazole alone as well as 29.5 days (control) and 34 days (elacridar

Figure 4.
Combination of mebendazole (MBZ) with elacridar (ELD). A, an IC_{50} curve of GL261 glioma cells with elacridar; $IC_{50} = 5.8$ μmol/L. B, inhibition of GL261 cells by mebendazole (0.25 μmol/L), elacridar (1 or 5 μmol/L), or the combination. Cells were incubated with the indicated drugs for 72 hours and the living cells were measured by the colorimetric assay. C, elacridar elevated the average B/P ratios of mebendazole in mice.

alone; Fig. 5B). Similarly, in the orthotopic D425 medulloblastoma xenograft model, the combination of elacridar with mebendazole increased the median survival to 77 days (Fig. 5D). This is a significant improvement from mebendazole only treatment with 52 days of survival and elacridar alone, which showed a marginal survival benefit of 9 days in this particular animal model.

A prolonged treatment course with elacridar and mebendazole was attempted; however, increased toxicity such as severe weight loss and mortality limited those studies (data not shown).

Discussion

The limited ability of cancer therapeutics to accumulate in the tumor is a major obstacle for improving brain cancer therapy (1). Although the pharmacokinetics of mebendazole for antiparasitic use have been studied in human and a number of animals, there are no CNS distribution data, especially in relation to efficacy against brain cancer (21). This is important for advancing mebendazole as a potential anti-brain cancer drug (3).

In this study, we demonstrate that mebendazole can reach the brain tissue in significant concentrations and with high brain to plasma ratios. Between 1 and 8 hours after the oral administration, MBZ-C maintained the brain levels above 0.767 μg/g (equivalent to 2.7 μmol/L), with a C_{max} of 2,016 μg/g (equivalent to 7.1 μmol/L). This exceeded the IC_{50} (4.3 μmol/L) of mebendazole on VEGFR2 kinase *in vitro* and the IC_{50} (0.11–1 μmol/L) in a series of glioma and medulloblastoma cell lines in tissue culture (3, 4). Furthermore, MBZ-C emerged as the most efficient polymorph, achieving an AUC_{0-24h} B/P ratio of 0.82. This is encouraging because temozolomide, the standard treatment for high-grade gliomas, was measured of having a B/P ratio of 0.408 in mice and a cerebrospinal fluid (CSF)/plasma ratio of 0.2 in human (22, 23). In our study, the distributions of mebendazole in the GL261 brain tumor and in the normal brain tissue did not differ significantly. It is worth mentioning that advanced growth of GL261 glioma results in substantial amount of blood in the tumor, similarly to other glioma models and a thorough perfusion was essential to eliminate the contamination of mebendazole from the blood. It is noteworthy that in some human trials mebendazole achieved lower plasma levels than in mice as the amino and hydroxy

metabolites reached 2- to 10-fold the plasma levels of the parental mebendazole (24, 25), which could indicate higher metabolic enzyme activities in human. Thus, much higher doses up to 200 mg/kg/d could be tolerated in human and should be used in future human brain tumor therapy (26).

Among the three polymorphs, MBZ-A showed no efficacy in GL261 glioma model, explained by the very low plasma presence at only 19% of AUC_{0-24h} measured with MBZ-C. MBZ-A's low bioavailability and inferior antitumor efficacy are in line with previous reports of its poor performance in antiparasitic applications (11, 13). In comparison, MBZ-B was able to reach 165% of MBZ-C's AUC_{0-24h} in the plasma, while showing a similar brain concentration demonstrated by the measurement at 6 hours. This could explain the elevated toxicity of MBZ-B in GL261 glioma-bearing mice as the anti-brain tumor efficacy remained essentially the same compared with MBZ-C. Thus, we suggest that MBZ-C is a better choice in brain tumor therapy. As a practical matter, the tablets made of MBZ-C should be stored under lower temperature (14), because the mebendazole tablets of Teva brand may have lost its efficacy under the standard RT condition within 3 years likely due to the conversion to polymorph A, although we do not know the original concentration of polymorph C in these tablets that used to be efficacious in our previous study (3).

Mebendazole's small size (295 daltons) and lipophilic property favor brain penetration (2). It is remarkable that other benzimidazoles tested so far, such as albendazole, thiabendazole, flubendazole, oxifendazole, and fenbendazole sharing similar physical properties, failed or only marginally improved the survival of GL261 glioma-bearing mice, even at higher doses than mebendazole (Supplementary Fig. S2; ref. 3). As we previously made the observation that fenbendazole in feed impaired the intake of the implantation of a medulloblastoma cell line in athymic nude mice (3), it only made a very marginal and statistically insignificant survival improvement in GL261 glioma model by gavaging 5 days after the implantation. There are several factors potentially contributing to the stark discrepancy in the brain tumor therapy with various benzimidazoles. For one as shown with mebendazole polymorph A, low bioavailability likely due to the poor absorption could be detrimental to the
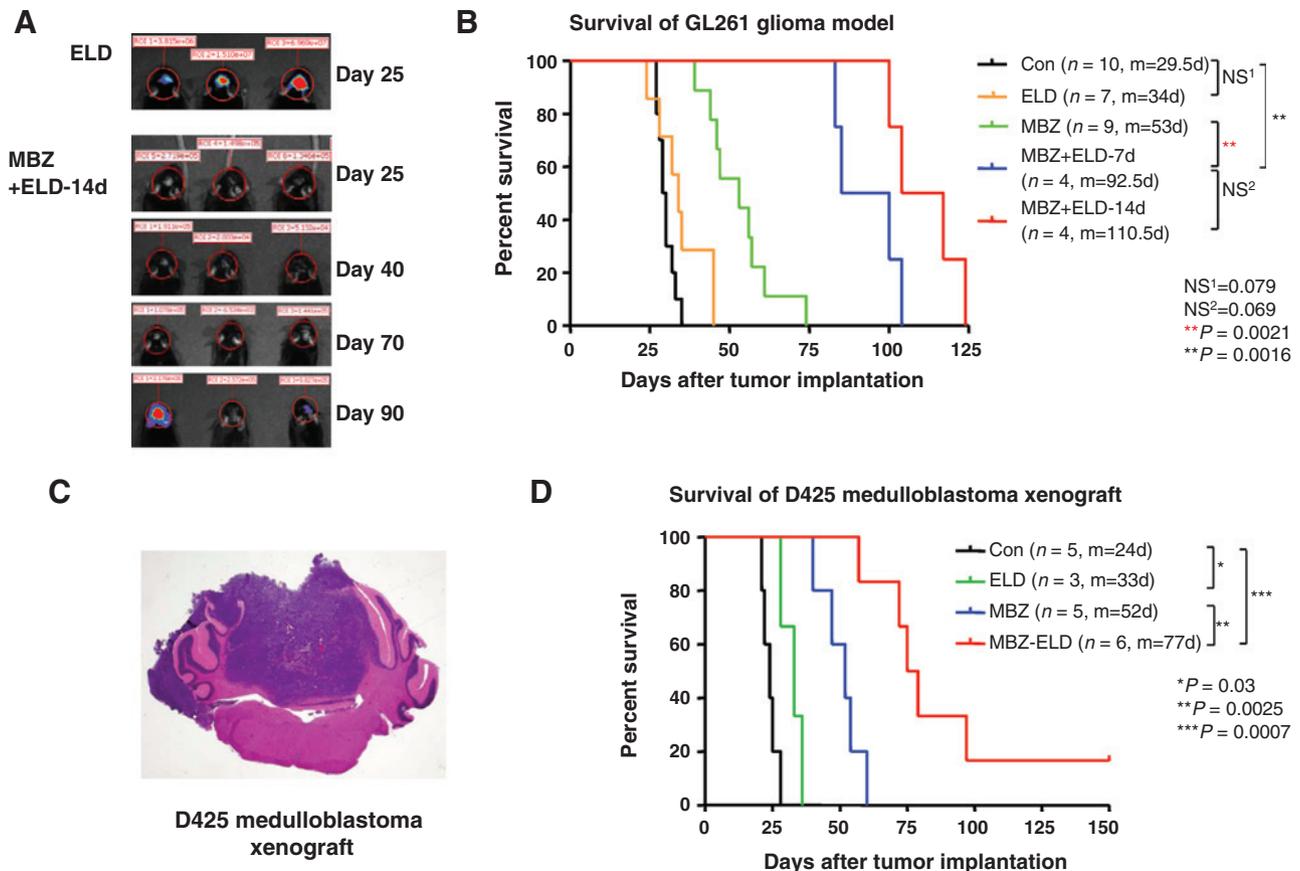
Figure 5.
Combination of mebendazole (MBZ) with elacridar (ELD) improved the efficacy. A and B, GL261 cells transfected with luciferase were implanted in C57BL6 mice and the treatments were initiated 5 days after the implantation. Elaridar was oral gavaged at 50 mg/kg 2 hours before the mebendazole administration (50 mg/kg) for the first 7 or 14 days of treatment. Thereafter, mebendazole was given 5 days a week at the same dose for the rest of the therapy. The elacridar alone group was gavaged with elacridar for 14 daily doses. Animals treated by mebendazole and elacridar were monitored by Xenogen for tumor luciferase signals starting from 25 days after the tumor implantation (A). C and D, D425 medulloblastoma cells were implanted in the mouse cerebellum and formed a cerebellar tumor [C, hematoxylin and eosin (H&E) staining]. Five days after the tumor implantation, mice were treated with vehicle (Con), 7 days of 50 mg/kg elacridar, 50 mg/kg MBZ-C alone (mebendazole), or 7 days of 50 mg/kg elacridar with 50 mg/kg MBZ-C (MBZ-ELD) following the same dosing regime in B.

therapeutic performance of this class of drugs. Second, the brain penetration of these benzimidazoles has not been well studied and could be insufficient for any significant therapeutic effects. Furthermore, mebendazole has been implicated in inhibiting multiple tyrosine kinases in recent reports, whereas albendazole showed lack of such ability, indicating differences in antitumor mechanisms among benzimidazoles (4, 7, 8).

P-glycoprotein (P-gp, ABCB1) is an ATP-binding cassette (ABC) transporter and plays an important role in limiting drug uptake into the brain. (27) Elacridar is a third-generation inhibitor of P-gp efflux transporters and also inhibits the breast cancer-resistant protein (BCRP and ABCG2) that is another key efflux transporter in BBB, as well as organic anion-transporting polypeptide 1B1 (OATP1B1), a hepatic uptake transporter (28, 29). Furthermore, elacridar has been found safe in phase I clinical trials (20). In this study, we investigated the combination of elacridar with mebendazole to potentially enhance its therapeutic efficacy. As results, we found that the combination greatly improved the survival in two orthotopic brain tumor models. However, in this limited study, the B/P ratio and brain AUC_{0-8h} of mebendazole did not show statistically significant

differences with coadministration of elacridar, despite its ability to significantly increase survival in brain cancer–bearing mice. When analyzing the metabolites, $MBZ-NH_2$, one of the two major metabolites in rodents and human (21), was significantly elevated in terms of B/P ratio (2.5-folds) and AUC_{0-8h} (2.4-folds) as a result of coadministration of elacridar. Also noticeable is our finding that $MBZ-NH_2$ was preferentially accumulated in the GL261 brain tumor versus the normal brain tissues. Although these data could indicate that $MBZ-NH_2$ is a potential substrate of P-gp and/or ABCG2, the significance of this finding is unclear at this point. A possible direct cytotoxic effect of $MBZ-NH_2$ appears unlikely as further testing displayed only a marginal cytotoxicity with cultured GL261 cells. The treatment of $MBZ-NH_2$ in GL261 brain tumor-bearing mice failed to show conclusive results (Supplementary Fig. S3). On the other hand, the added cytotoxic effects of mebendazole and elacridar could also contribute to the enhanced efficacy. In D425 medulloblastoma cells, elacridar at 5 µmol/L significantly enhanced the cytotoxicity of mebendazole in vitro (Supplementary Fig. S4). Further investigations include the study of mebendazole and elacridar interactions, particularly the

potential substrate profile of efflux transporters with mebendazole, to better understand, and thereby improve the combination with mebendazole.

In conclusion, MBZ-C is the most efficacious polymorph in brain tumor therapy. The combination of MBZ-C with elacridar can greatly improve the efficacy, and this combination should be studied for safety in future phase I clinical trials of high-grade glioma and/or medulloblastoma.

Disclosure of Potential Conflicts of Interest

R.-Y. Bai, V. Staedtke, A.D. Joshi, and G.J. Riggins are listed as co-inventors on a provisional patent application on an improved formulation of mebendazole and certain drug combinations with mebendazole that is owned by Johns Hopkins University and managed in accordance with its conflict-of-interest policy. No potential conflicts of interest were disclosed by the other authors.

Authors' Contributions

Conception and design: R.-Y. Bai, V. Staedtke, G.J. Riggins
Development of methodology: R.-Y. Bai, V. Staedtke, M.A. Rudek
Acquisition of data (provided animals, acquired and managed patients, provided facilities, etc.): R.-Y. Bai, V. Staedtke, T. Wanjiku, M.A. Rudek, A. Joshi

References

1. Bai RY, Staedtke V, Riggins GJ. Molecular targeting of glioblastoma: drug discovery and therapies. Trends Mol Med 2011;17:301–12.
2. Chico LK, Van Eldik LJ, Watterson DM. Targeting protein kinases in central nervous system disorders. Nat Rev Drug Discov 2009;8:892–909.
3. Bai RY, Staedtke V, Aprhys CM, Gallia GL, Riggins GJ. Antiparasitic mebendazole shows survival benefit in 2 preclinical models of glioblastoma multiforme. Neuro Oncol 2011;13:974–82.
4. Bai RY, Staedtke V, Rudin CM, Bunz F, Riggins GJ. Effective treatment of diverse medulloblastoma models with mebendazole and its impact on tumor angiogenesis. Neuro Oncol 2015;17:545–54.
5. Doudican N, Rodriguez A, Osman I, Orlow SJ. Mebendazole induces apoptosis via Bcl-2 inactivation in chemoresistant melanoma cells. Mol Cancer Res 2008;6:1308–15.
6. Doudican NA, Byron SA, Pollock PM, Orlow SJ. XIAP downregulation accompanies mebendazole growth inhibition in melanoma xenografts. Anticancer Drugs 2013;24:181–8.
7. Dakshanamurthy S, Issa NT, Assefnia S, Seshasayee A, Peters OJ, Madhavan S, et al. Predicting new indications for approved drugs using a proteochemometric method. J Med Chem 2012;55:6832–48.
8. Nygren P, Fryknas M, Agerup B, Larsson R. Repositioning of the anthelmintic drug mebendazole for the treatment for colon cancer. J Cancer Res Clin Oncol 2013;139:2133–40.
9. Larsen AR, Bai RY, Chung JH, Borodovsky A, Rudin CM, Riggins GJ, et al. Repurposing the antihelmintic mebendazole as a hedgehog inhibitor. Mol Cancer Ther 2015;14:3–13.
10. Liebenberg W, Dekker TG, Lotter AP, de Villiers MM. Identification of the mebendazole polymorphic form present in raw materials and tablets available in South Africa. Drug Dev Ind Pharm 1998;24:485–8.
11. Rodriguez-Caabeiro F, Criado-Fornelio A, Jimenez-Gonzalez A, Guzman L, Igual A, Perez A, et al. Experimental chemotherapy and toxicity in mice of three mebendazole polymorphic forms. Chemotherapy 1987;33:266–71.
12. Swanepoel E, Liebenberg W, de Villiers MM. Quality evaluation of generic drugs by dissolution test: changing the USP dissolution medium to distinguish between active and non-active mebendazole polymorphs. Eur J Pharm Biopharm 2003;55:345–9.
13. Charoenlarp P, Waikagul J, Muennoo C, Srinophakun S, Kitayaporn D. Efficacy of single-dose mebendazole, polymorphic forms A and C, in the treatment of hookworm and Trichuris infections. Southeast Asian J Trop Med Public Health 1993;24:712–6.
14. Brits M, Liebenberg W, de Villiers MM. Characterization of polymorph transformations that decrease the stability of tablets containing the WHO essential drug mebendazole. J Pharm Sci 2010;99:1138–51.
15. Bai RY, Staedtke V, Lidov HG, Eberhart CG, Riggins GJ. OTX2 represses myogenic and neuronal differentiation in medulloblastoma cells. Cancer Res 2012;72:5988–6001.
16. Sane R, Agarwal S, Elmquist WF. Brain distribution and bioavailability of elacridar after different routes of administration in the mouse. Drug Metab Dispos 2012;40:1612–9.
17. DiResta GR, Lee J, Lau N, Ali F, Galicich JH, Arbit E. Measurement of brain tissue density using pycnometry. Acta Neurochir Suppl 1990;51:34–6.
18. Bailer AJ. Testing for the equality of area under the curves when using destructive measurement techniques. J Pharmacokinet Biopharm 1988;16:303–9.
19. Yuan J. Estimation of variance for AUC in animal studies. J Pharm Sci 1993;82:761–3.
20. Werle M, Takeuchi H, Bernkop-Schnurch A. New-generation efflux pump inhibitors. Expert Rev Clin Pharmacol 2008;1:429–40.
21. Dayan AD. Albendazole, mebendazole and praziquantel. Review of nonclinical toxicity and pharmacokinetics. Acta Trop 2003;86:141–59.
22. Zhou Q, Gallo JM. Differential effect of sunitinib on the distribution of temozolomide in an orthotopic glioma model. Neuro Oncol 2009;11:301–10.
23. Ostermann S, Csajka C, Buclin T, Leyvraz S, Lejeune F, Decosterd LA, et al. Plasma and cerebrospinal fluid population pharmacokinetics of temozolomide in malignant glioma patients. Clin Cancer Res 2004;10:3728–36.
24. Luder PJ, Siffert B, Witassek F, Meister F, Bircher J. Treatment of hydatid disease with high oral doses of mebendazole. Long-term follow-up of plasma mebendazole levels and drug interactions. Eur J Clin Pharmacol 1986;31:443–8.
25. Braithwaite PA, Roberts MS, Allan RJ, Watson TR. Clinical pharmacokinetics of high dose mebendazole in patients treated for cystic hydatid disease. Eur J Clin Pharmacol 1982;22:161–9.
26. Messaritakis J, Psychou P, Nicolaidou P, Karpathios T, Syriopoulou B, Fretzayas A, et al. High mebendazole doses in pulmonary and hepatic hydatid disease. Arch Dis Child 1991;66:532–3.
27. Redzic Z. Molecular biology of the blood–brain and the blood-cerebrospinal fluid barriers: similarities and differences. Fluids Barriers CNS 2011;8:3.
28. Shukla S, Ohnuma S, Ambudkar SV. Improving cancer chemotherapy with modulators of ABC drug transporters. Curr Drug Targets 2011;12:621–30.
29. Oostendorp RL, van de Steeg E, van der Kruijssen CM, Beijnen JH, Kenworthy KE, Schinkel AH, et al. Organic anion-transporting polypeptide 1B1 mediates transport of Gimatecan and BNP1350 and can be inhibited by several classic ATP-binding cassette (ABC) B1 and/or ABCG2 inhibitors. Drug Metab Dispos 2009;37:917–23.

Clinical Cancer Research

Brain Penetration and Efficacy of Different Mebendazole Polymorphs in a Mouse Brain Tumor Model

Ren-Yuan Bai, Verena Staedtke, Teresia Wanjiku, et al.

Updated version	Access the most recent version of this article at: doi:10.1158/1078-0432.CCR-14-2681
Supplementary Material	Access the most recent supplemental material at: http://clincancerres.aacrjournals.org/content/suppl/2015/04/14/1078-0432.CCR-14-2681.DC1

E-mail alerts	Sign up to receive free email-alerts related to this article or journal.
Reprints and Subscriptions	To order reprints of this article or to subscribe to the journal, contact the AACR Publications Department at pubs@aacr.org.
Permissions	To request permission to re-use all or part of this article, use this link http://clincancerres.aacrjournals.org/content/early/2015/06/03/1078-0432.CCR-14-2681. Click on "Request Permissions" which will take you to the Copyright Clearance Center's (CCC) Rightslink site.